Final Report to the DOE on the Construction of the High Energy Resolution Spectrometer (HERS) Endstation on Beamline 10.0.1.1 of the Advanced Light Source

by
Scott Kellar and Zhi-Xun Shen
Stanford University
Stanford, CA 94305

This report details the successful construction of the high energy-resolution spectrometer (HERS) endstation at the Advanced Light Source, DOE contract DE-FG03-96ER45594. This endstation was designed to study highly correlated-materials, including the high-T_c superconductors (HTS) with unprecedented resolution. As many feel that the most useful clues to understanding these fascinating materials will come from angle-resolved photoemission data (ARPES) the 100 fold increase in momentum resolution and data collection efficiency afforded by this new endstation will make significant breakthroughs in HTS research possible. Indeed, HERS has already provided new insights into the HTS materials and the extremely intriguing Stripe phase. The HERS construction consisted of four important subsections. The first is the vacuum vessel and sample transfer system. Because of the reactive nature of the HTS surfaces, reliable data requires very good vacuum in the middle to low 10^{-11} Torr range. The second important aspect is, of course, the electron energy analyzer. We purchased a commercially produced analyzer from Gammadata Scienta, AB, the performance of which is detailed below. Perhaps the most important aspect of any such system is the sample manipulator. Because no suitable commercial product is available, we have designed and successfully built a cryogenic manipulator with very accurate motion over five degrees of freedom. Lastly, this report will detail the construction of the electron spin analyzer (ESA).

Figure 1 is a photograph of the HERS endstation as it is installed on ALS beamline 10.0.1.1. The vacuum chamber is composed of three independent vessels separated by valves. The main chamber, where the electron energy analyzer is mounted rotates 120° about the incoming synchrotron photon beam. Because the radiation from the storage ring is polarized in the plane of the ring, this rotation allows one to vary the polarization incident on the target from s to p while maintaining a constant emission angle from the sample. Two differentially pumped rotary seals mounted to the chamber allow the rotation while maintaining excellent vacuum. The chamber base pressure is less than 3 x 10^{-11} torr, and there is no appreciable pressure change when the analyzer is rotated. An X-ray source mounted in this chamber provides opportunities for studying samples without the synchrotron beam. The rotating chamber is separated from the secondary analysis chamber by a vacuum valve. The secondary analysis chamber is equipped with a low

DISCLAIMER

DISCLAIMER

Portions of this document may be illegible in electronic image products. Images are produced from the best available original document.

energy electron diffraction (LEED) apparatus. In addition, this section of the chamber has the ports necessary for the future installation of a scanning tunneling microscope (STM) as well as ports for a surface magneto-optical Kerr effect (SMOKE) apparatus. Again, the secondary analysis chamber is separated from the prep chamber by a vacuum valve. The prep chamber contains sample preparation tools, including an ion sputtering gun, cleavers, and evaporation sources.

Because of the stringent vacuum quality required for photoemission from the HTS samples and because most samples cannot be baked special attention was placed on the sample transfer system. A CAD drawing of this unit and its constituent parts is shown in Fig. 2. It consists of three intermediate vacuum stages. All the parts are identical and repeated for each stage. This design accomplishes several important adjectives. First, by passing through each successive stage takes the samples into cleaner and cleaner vacuum. In practice, it is possible to transfer a fresh sample from atmosphere through the successive stages of the load lock system and on to the cryostat in 2 hours without baking and maintaining the prep chamber pressure of 5 X 10-11 Torr. The second important aspect is that this system allows a tremendous amount of sample "parking", so that we can always have sample ready to make the most efficient use of the available beamtime. The sample transfer and Load Lock system is of paramount importance to the success of the HERS endstation.

The electron energy analyzer is a commercial unit purchased from Gammadata Scienta AB. As Figs. 3A and 3B show, the energy resolution from this instrument is excellent. Fig. 3A is the photoemission spectrum of the Ar $3p_{3/2}$ core level, excited with 25 eV photons from beamline 10.0.1.1. The full width at half maximum of the peak is 8 meV. Accounting for the natural line width and Doppler broadening of the Ar 3p line, the total contribution from the beamline and the analyzer to the peak width is 3 meV. In Fig. 3B we plot the Fermi-edge signal from a poly-crystalline gold sample at 10 K. After deconvolving the thermal effects which broaden the line by 4.4KT or 4 meV at 10 K, The combined resolution of the beamline and the analyzer is 7 meV.

In addition to the excellent energy resolution the analyzer also demonstrated very good angular resolution. When operating in the angular mode, the analyzer lens system focus changes so that the lens' diffraction plane is at the entrance slit to the analyzer, effectively converting angular information into positional information along the slit. The hemispherical detector maintains this angular information while separating the electrons by kinetic energy. Using the proper image-capturing equipment we can at one time collect and energy analyze electrons leaving the sample within a cone of ± 7° with 0.2° resolution. This angular resolution is an order of magnitude increase over previous equipment. In Fig. 4, we show the results of the angular mode testing. The electron

source is a thin wire illuminated by the synchrotron beam. This wire is parallel to a slit array positioned 25 mm above it. With slits which are 100 μm wide and 500 μm a part, the angular width is 0.3° and the spacing 1.0°. Accounting for the width of the source, we determine the angular resolution to be ± 0.15°. Most importantly, as can be seen in Fig. 4, the angular magnification is constant over the 14° acceptance of the lens and over a wide kinetic energy range, even at energies approaching the pass energy. While the intensity is slightly uneven over several channels, we believe this is an artifact due to inhomogeneous graphite coating on the slit array.

The manipulator consists of two important parts. The first is the x,y,z stage. For this part we made use of existing technology and purchased a commercial mill table. The mill, while quite large, works very well in this application allowing very precise sample movements of 0.001" over the 37" of travel from the sample prep chamber to the analysis position in the main chamber. The second aspect of the manipulator is the rotary motion. Polar angle rotation is accomplished by a differentially pumped rotary feedthrough to which the liquid helium cooled cryostat is mounted. The azimuthal rotation about the surface normal is cable driven through a standard rotary feedthrough. The samples are held onto the cryostat by a radial spring and then rotated by the cable drive. The rotational accuracy for both axes is 0.2°. With the LHe cooled cryostat the sample temperature can be controlled from 10 K to 450 K with better than one degree accuracy.

The electron spin analyzer (ESA) Fig. 5 is machined, assembled, and in being tested. After reviewing the literature and the "State of the Art" for mini-Mott type ESA's we decided that there was significant room for improvement. When compared with older designs the HERS ESA incorporates a sophisticated lens system, which allows a very large acceptance aperture, 2-mm x 10-mm, from the exit plane of the electron energy analyzer to be focussed to a sub-millimeter diameter spot at the scattering target. The lens, meaning greater throughput. The second is the more sophisticated lens system has greatly reduced aberrations leading to a considerably smaller spot size on the scattering target. Lastly, the lens system produces far fewer scattered electrons, which means a cleaner signal and improved signal to noise ratio. Because the spin detection is a very low cross-section event, we will need these advances to achieve our goal of spin resolved photoemission spectra with "kT", or 25-meV resolution. By our estimates the new ESA will be at least 30 times more efficient than conventional designs. Additionally, because of the 90° deflector in the design we will be able to measure all three orthogonal components of the electron spin. To date the ESA is performing well in testing with a spot size at the scattering target of less than 250-μm. we will incorporate the ESA into the rest of the HERS system soon.

Our recent paper published in *Science* (**286**, 268 (1999)) is an excellent example of just what a powerful machine we have constructed at the ALS. Fig.6 represents nearly 700 individual photoemission spectra collected from the stripe compound, Nd-LSCO. All the spectra were collected with a combined energy resolution of 18 meV and angular resolution of ±0.15°, in only three hours. Because of the extremely reactive nature of the surface, the short data collection time was absolutely necessary to complete a meaningful experiment. Furthermore, the unique energy range of beamline 10.0.1.1 allowed us to choose a photon-energy with which we can span the Nd-LSCO brillioun zone with one 14° snapshot from the analyzer. This study was the first on the electronic structure of this extremely intriguing class of materials exhibiting the stripe phase. This data and the subsequent analysis gave us profound new insights into the nature of superconductivity and the stripe phase. Just what the machine was designed and built to do.

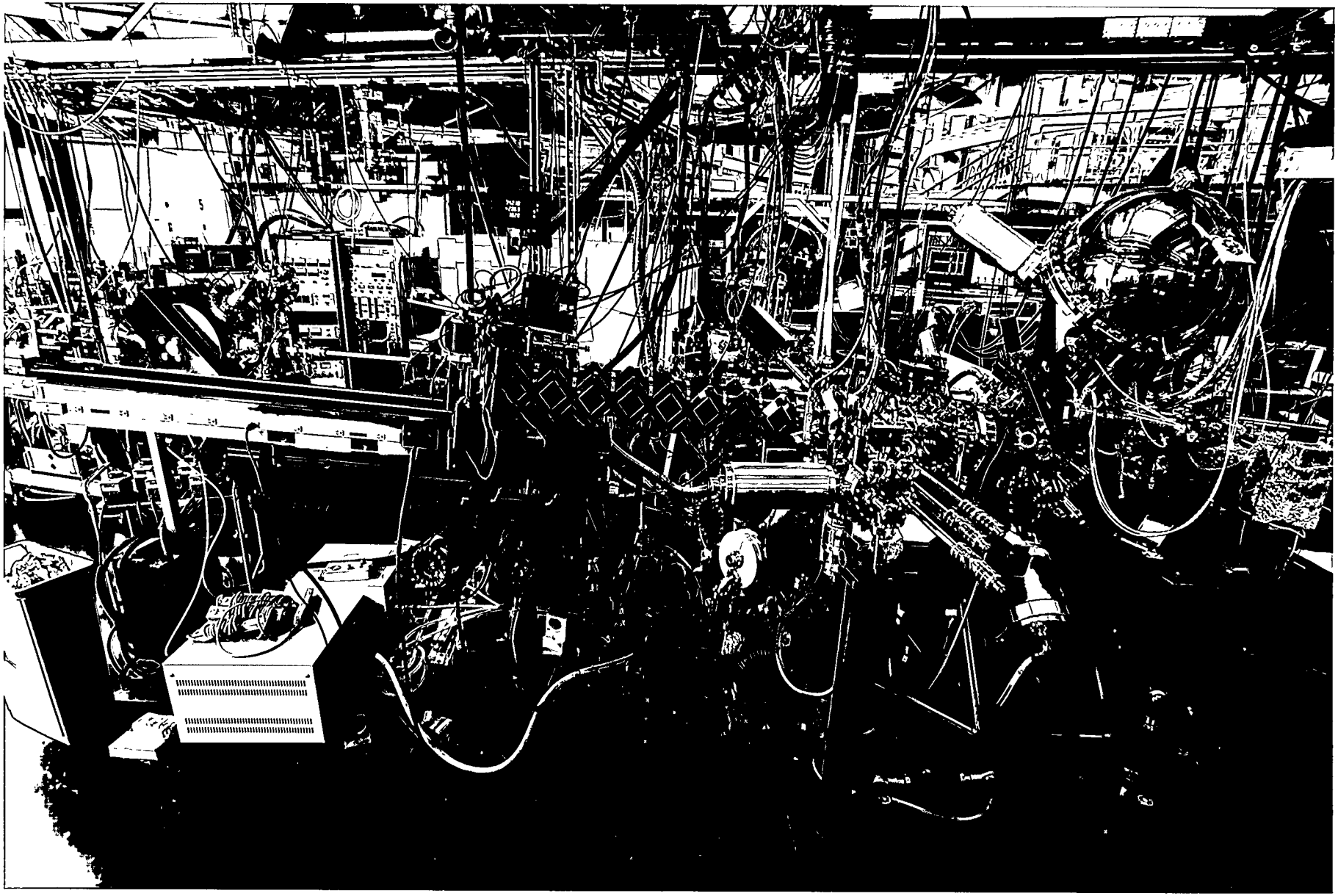

FIG 1.

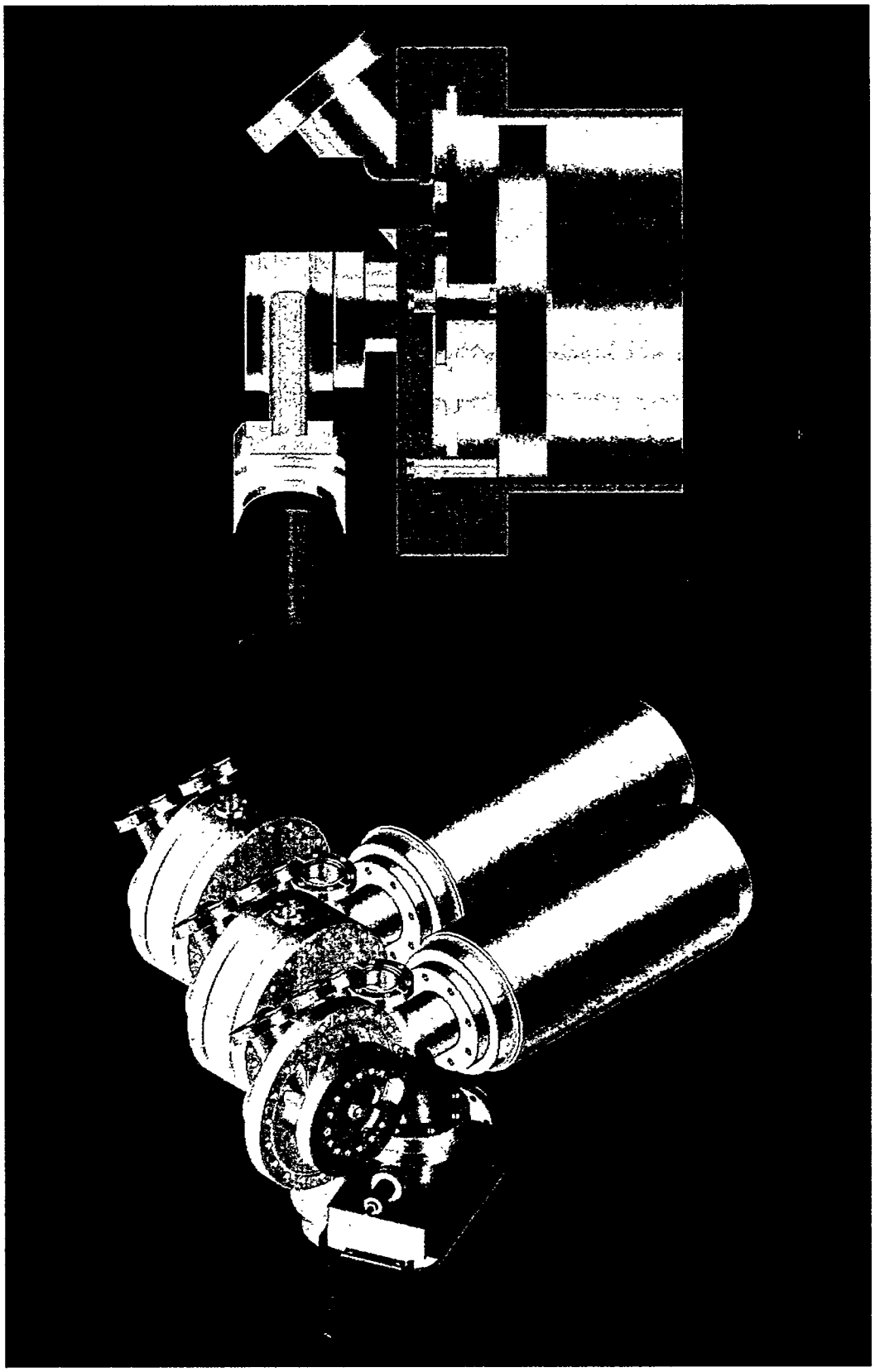

Figure 2 A & 2B.

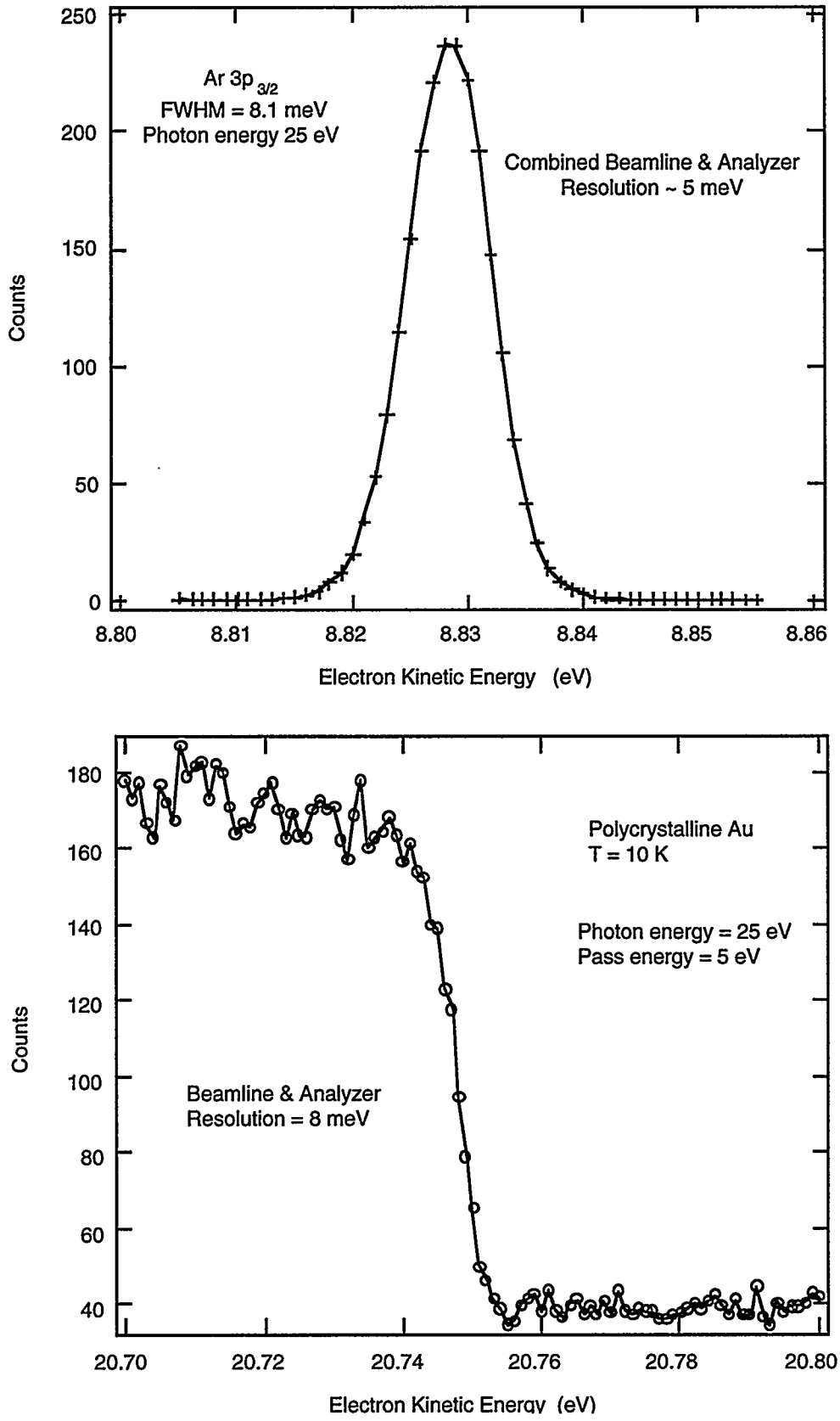
Ar 3p 3/2
FWHM = 8.1 meV
Photon energy 25 eV
Combined Beamline & Analyzer
Resolution ~ 5 meV
Counts
Electron Kinetic Energy (eV)
Polycrystalline Au
T = 10 K
Photon energy = 25 eV
Pass energy = 5 eV
Beamline & Analyzer
Resolution = 8 meV
Counts
Electron Kinetic Energy (eV)

Figure 3A & 3B

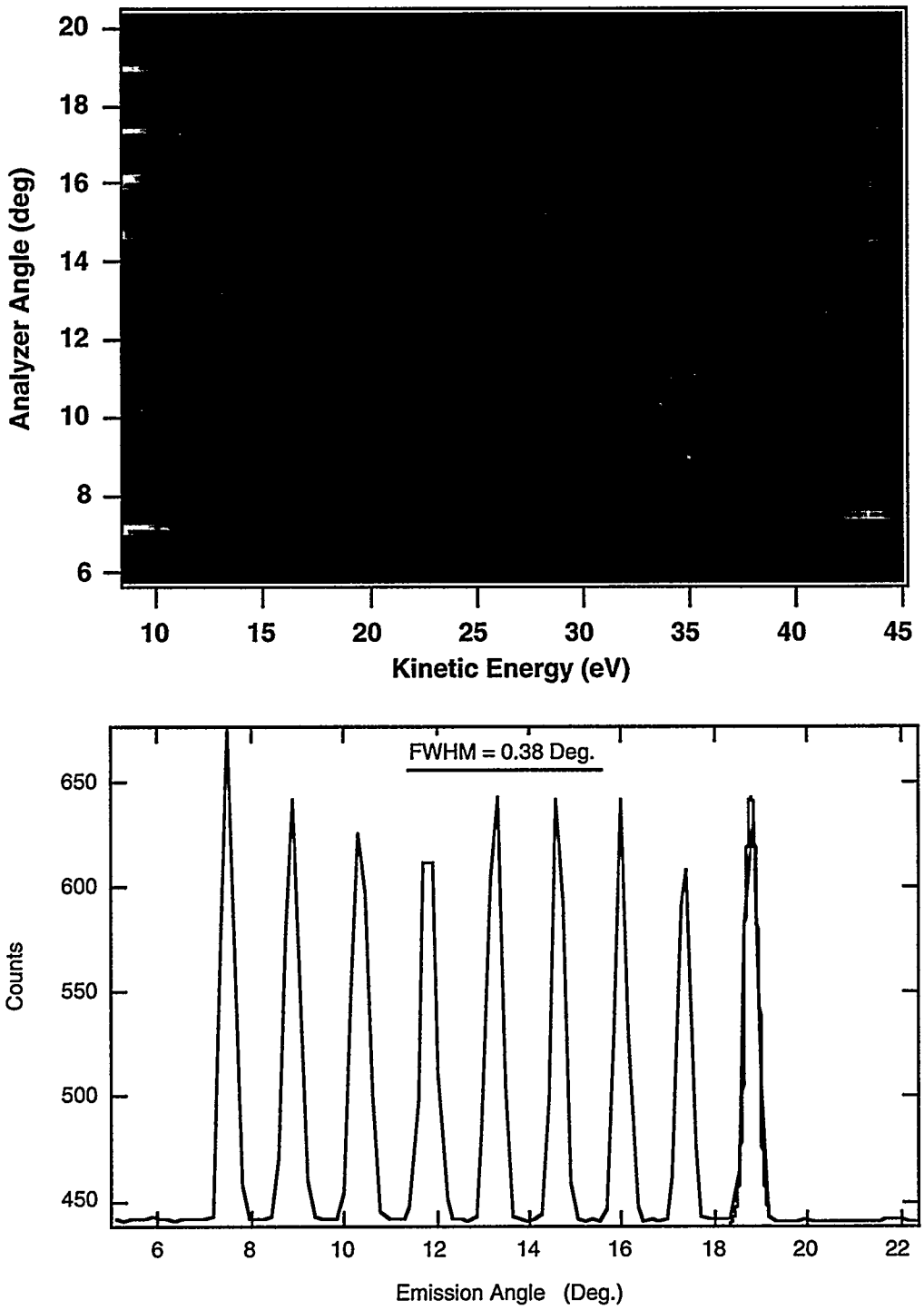
Analyzer Angle (deg)
20
18
16
14
12
10
8
6
10
15
20
25
30
35
40
45
Kinetic Energy (eV)
FWHM = 0.38 Deg.
Counts
650
600
550
500
450
6
8
10
12
14
16
18
20
22
Emission Angle (Deg.)

Figure 4A & 4B

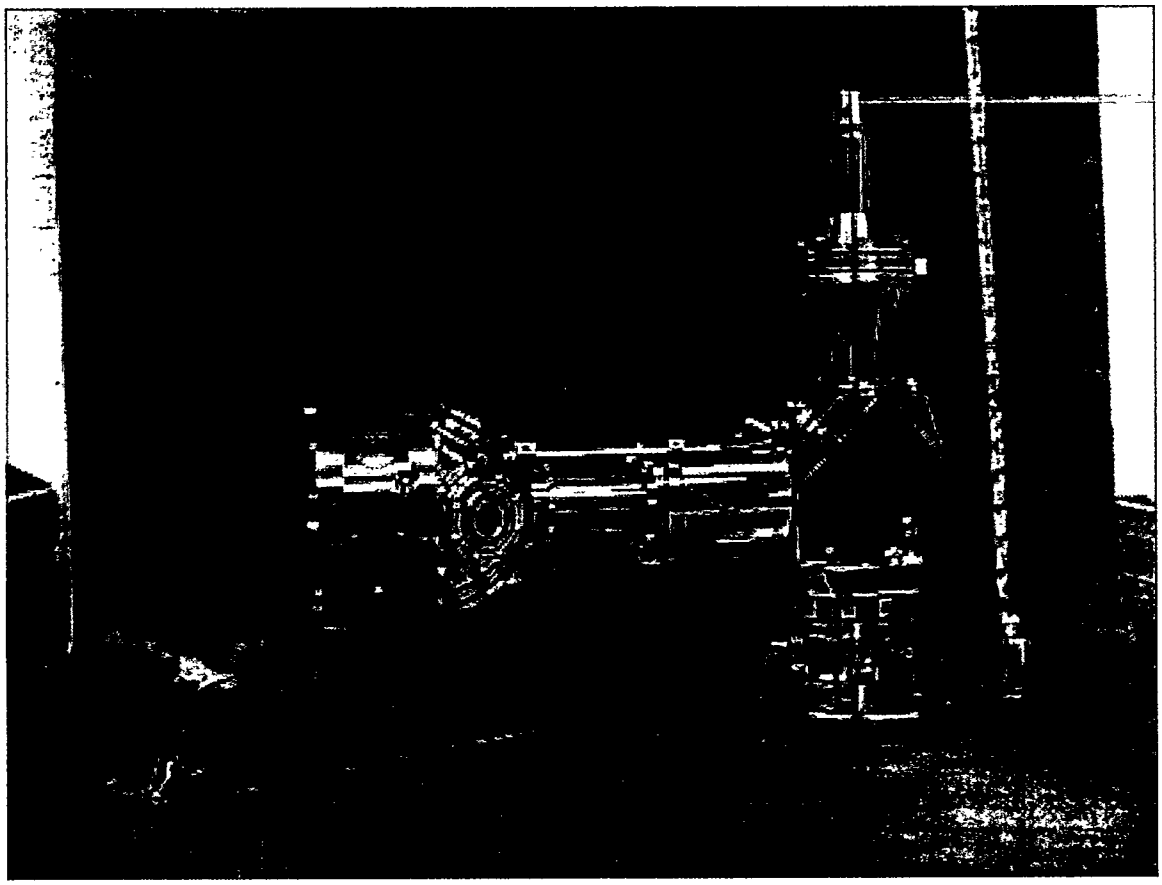

Figure 5.

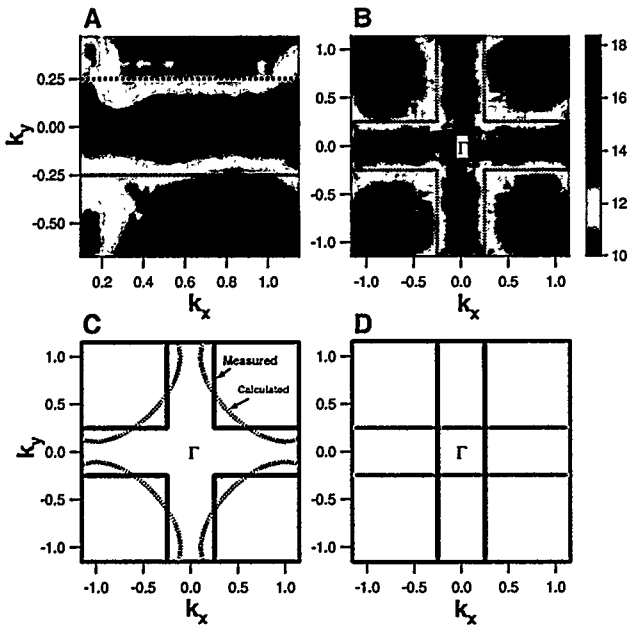
A
B
C
D
0.25
0.00
-0.25
-0.50
k_y
0.2 0.4 0.6 0.8 1.0
k_x
1.0
0.5
0.0
-0.5
-1.0
-1.0 -0.5 0.0 0.5 1.0
k_x
18
16
14
12
10
Measured
Calculated
Γ
Γ

FIG 6.

FIGURE CAPTIONS

Figure 1. A photograph of the HERS endstation installed on Beamline 10.0.1.1 at the Advanced Light Source.

Figure 2. A. One of the repeating units that comprise the sample transfer/load lock system. Each wheel has space for 13 sample holders, shown in gold. B. The assembled sample transfer system showing all three stages. The vacuum is progressively better in each stage allowing sample transfer from atmosphere to 5×10^{-11} Torr without baking in two hours

Figure 3. A. The photoemission spectrum of the Ar 3p line measured with the HERS endstation and 25 eV photons from Beamline 10.0.1.1. The combined resolution of the beamline and analyzer is better than 4 meV.
B. The photoemission spectrum of the Fermi-edge from a polycrystalline Au foil at 10 K. The combined resolution calculated from this spectrum is 8 meV.

Figure 4. Results of the angular resolution testing. A. This image is made by electrons passing through the slit array at different angles collected simultaneously in parallel by the analyzer. As can be seen in the image the magnification is very constant over a large kinetic energy range. B. A line cut through the image in A showing the analyzer resolution to be about ±0.15°.

Figure 5. Photograph of the assembled ESA.

Figure 6. The spectral weight integrated within 500 meV of the Fermi level, as a funciton of K_x and K_y. (**A**) is obtained directly from the raw data, whereas (**B**) is obtained by four-fold symmetrizing the raw data in (A). The dotted line in (A) and (B) define the regions where the spectral weight is mainly concentrated. (**C**) depicts the underlying Fermi surface (solid line) obtained from (B) that encloses the high spectral weight region. The calculated Fermi surface for the 2D CuO_2 plane is also shown (dotted lines) for comparison. (D) depicts the Fermi surface expected from two perpendicular 1D stripe domains in the 1D interpretation. Γ is the center of the BZ.